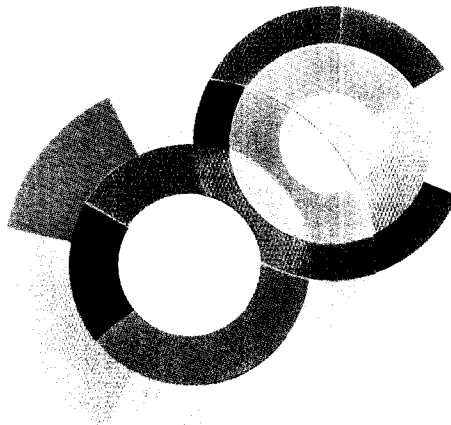
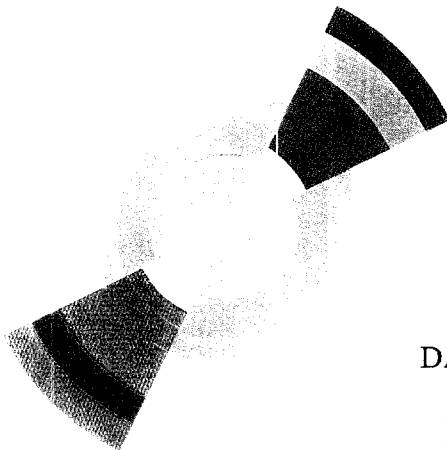


5159830



DAPNIA/ 98-01

June 1998

DEVELOPMENT OF FAST GASEOUS DETECTOR  
« MICROMEGAS » WCC 1998

**G. Barouch, A. Bay, S. Bouchigny, G. Charpak, J. Derré, F. Didierjean,  
J.-C. Faivre, Y. Giomataris, C. Kochowski, F. Kunne, J.-M. Le Goff,  
F. Lehar, Y. Lemoigne, S. Loucatos, J.-C. Lagnol, A. Magnon,  
J.-P. Perroud, S. Platchkov, G. Puill, Ph. Rebourgeard,  
D. Thers, H. Zaccane**

**DAPNIA**

*Invited Talk presented by Y. Giomataris at the 8<sup>th</sup> Vienna Wirechamber Conference,  
Wien (Austria), February 23-27 1998  
Submitted to Nuclear Instruments & Methods in Physics Research A*

Le DAPNIA (Département d'Astrophysique, de physique des Particules, de physique Nucléaire et de l'Instrumentation Associée) regroupe les activités du Service d'Astrophysique (SAp), du Département de Physique des Particules Élémentaires (DPhPE) et du Département de Physique Nucléaire (DPhN).

Adresse : DAPNIA, Bâtiment 141  
CEA Saclay  
F - 91191 Gif-sur-Yvette Cedex

# Development of a fast gaseous detector "Micromegas" WCC 1998

G. Barouch<sup>a</sup>, A. Bay<sup>b</sup>, S. Bouchigny<sup>a</sup>, G. Charpak<sup>c</sup>, J. Derré<sup>a</sup>,  
F. Didierjean<sup>d</sup>, J.-C. Faivre<sup>a</sup>, Y. Giomataris<sup>a</sup>, C. Kochowski<sup>a</sup>,  
F. Kunne<sup>a</sup>, J.-M. Le Goff<sup>a</sup>, F. Lehar<sup>a</sup>, Y. Lemoigne<sup>a</sup>,  
S. Loucatos<sup>a</sup>, J.-C. Lugol<sup>a</sup>, A. Magnon<sup>a</sup>, J.-P. Perroud<sup>b</sup>,  
S. Platchkov<sup>a</sup>, G. Puill<sup>a</sup>, Ph. Rebourgeard<sup>a</sup>, D. Thers<sup>a</sup> and  
H. Zacccone<sup>a</sup>

<sup>a</sup>*CEA/Saclay, DAPNIA, 91191 Gif-sur-Yvette Cedex, France*

<sup>b</sup>*Lausanne University, IPN, BSP, 1015 Dorigny, Switzerland*

<sup>c</sup>*CERN/AT, Geneva, Switzerland*

<sup>d</sup>*EURISYS Mesures, 1 Chemin de la roseraie, Lingolsheim, 67834 Tanneries  
Cedex, France*

Several  $15 \times 15 \text{ cm}^2$  gaseous Micromegas chambers (MICRO MESH Gaseous Structure) which consist of a conversion gap and an amplification gap separated by a thin grid have been extensively tested in low intensity 10 GeV/c pion beam and high intensity, up to  $5 \times 10^5 \text{ Hz} / \text{mm}^2$ , 100 GeV/c muon beam. The detector behavior with respect of many parameters has been studied; conversion gap of 1 mm and 3 mm, amplification gap of 50 microns and 100 microns, effect of an external magnetic field and many different filling gases. So far no effect of the magnetic field up to 1.3 T has been observed. The gas mixture Argon + Cyclohexane appears to be very suitable with gains above  $10^5$  and a full efficiency plateau of 50 V at 340 V. With a conversion gap as small as 1 mm and an electronics with a threshold at 5000 electrons the efficiency reaches 96%. With the addition of  $\text{CF}_4$  a time resolution of 5 ns (RMS) has been obtained. A spatial resolution better than 60 microns has been observed with anode strips of 317 microns pitch and was explained by transverse diffusion in the gas. Simulations show that with a pitch of 100 microns and the appropriate gas a resolution of 10 microns is within reach.

This development leads to a new generation of cheap position sensitive detectors which would permit high precision tracking or vertexing close to the interaction region, in very high-rate environments.

## 1 Introduction

Micromegas [1] is a new gaseous detector based on simple geometry with planar electrodes. It consists of a conversion gap in which radiations liberate ionization electrons and of a thin amplification gap. The two regions are separated by a thin ( $3\ \mu\text{m}$ ) grid. The free electrons drift into the amplification gap where printed electrodes of any shape collect the electrons from the avalanche.

We had come to the conclusion, in our preliminary tests [2], that it is possible to build chambers of sizes adapted to the future high luminosity detectors, with high count rates capability and good time and space resolution.

The first beam tests were made with chambers filled with gases known for their high resistance against aging in intense beams: Argon + Dimethylether (DME). Then, after a year of intensive beam and laboratory tests, we concluded that the detector is radiation hard: even using other gas mixtures we didn't observe any degradation due to the aging of the detector. This was done with our initial chambers, with an amplification gap of  $100\ \mu\text{m}$  and a drift gap of 3 mm.

Our research was then enlarged to a systematic study of gases. We found that Argon + Cyclohexane vapors present a significant improvement in efficiency and plateau width. A search for the best time resolution has shown that adding  $\text{CF}_4$  increases substantially the electron drift velocity and yields a time resolution around 5 ns (RMS), even the efficiency was reduced.

The localization performance of the detector has been studied using printed strips with  $317.5\ \mu\text{m}$  pitch. With Argon and DME the spatial resolution was found to be  $60\ \mu\text{m}$ , limited by the transverse diffusion of the gas.

An amplification gap of  $50\ \mu\text{m}$ , which is easy to achieve with the actual technology we have developed, gives an improvement in the time jitter. To reduce the degradation of the spatial resolution of the inclined tracks, we have also tested that it is possible to work with a conversion gap of only 1 mm as the efficiency reaches 96%.

Chambers were tested at muon rates of  $2 \times 10^8$  per burst of 2 s of the CERN SPS over an area of  $2\ \text{cm}^2$ . We present these results which are a step in a more extended search for the improvement of this detector and its adaptation to various problems in particle physics.

## 2 Detector description

### 2.1 Geometry

A detailed description of Micromegas is given in [1]. Our tests were performed with  $15 \times 15 \text{ cm}^2$  chambers with a conversion gap of 3 mm, an amplification gap of 100 or 50  $\mu\text{m}$  and a strip pitch of 317.5  $\mu\text{m}$  with a spacing of 70  $\mu\text{m}$ . The parallelism between the micromesh grid and the anode is maintained by spacers of 200  $\mu\text{m}$  diameter, every 2 mm. They are printed on a thin epoxy substrate by conventional lithography of a photoresistive film. This is a very cheap and easy process. The height of the spacers is 100 or 50  $\mu\text{m}$ , and other spacings are also possible. Thin Kapton foil can be used instead of epoxy as substrate in order to reduce matter thickness. Developments in this way have already started.

### 2.2 Electrical Properties

The electric field is homogeneous inside both the conversion and the amplification gap. It only exhibits a funnel like shape very close to the openings of the microgrid: field lines are compressed towards the middle of the openings into a small diameter of the order of a few microns, depending on the electric field ratio between the two gaps. All the electrons liberated in the conversion gap by the ionizing radiation are focused into the multiplication gap. Fig. 1 displays details of equipotentials near the grid used in the present tests (50  $\mu\text{m}$  opening pitch).

An interesting property of Micromegas is that small variations of the amplification gap, due to mechanical defects, are compensated by an inverse variation of the amplification factor. As shown in Fig. 2, for a given voltage applied in a thin parallel plate chamber, the gain as a function of the gap width presents a maximum around 50 to 100 microns. Micromegas which operates in this region is therefore not sensitive to defects of flatness and is optimal for parallel-plate avalanche mode, resulting in a rather large dynamic range for the amplification before breakdown.

### 2.3 Signal development and electronics

The signal induced on the anode strips is a sum of the electron and ion signal. The charge induced by electrons and ions are equal. But, respect to the ions,

the drift velocity of the electrons is 100 times bigger, so the current pulse is 100 times shorter and 100 times higher.

Using a low-noise charge preamplifier, the charge signal is mainly due to the positive ion drift to the micromesh electrode, which takes place typically within 100 ns, depending on the width of the amplification gap. Fig. 3 shows signals coming out from a charge-sensitive preamplifier for an Argon + 10% Isobutane gas mixture. A reduction of the amplification gap from 100 to 50 microns reduces the signal rise time by a factor 3. So, for the latter case, shaping of the signal around 50 ns allows to catch the full induced charge and therefore permits a comfortable operation of the detector at moderate gains of the order of 3000, enough low to prevent sparks in the detector.

As far as the current signal is concerned the calculation exhibits a very fast rise of the current, less than 1 ns, and a tail due to the ion drift. The very fast electron signal is quite difficult to catch, but is within reach with present electronics. It is illustrated in Fig. 4 showing signals taken using a commercially available Lecroy-MQS104A chip (10 ns rise), during a high rate beam test in the SPS at CERN. The figure shows two signals, simultaneously taken from two detectors with respectively 100 and 50 microns amplification gap. With the 100 microns gap the signal has a fast rise due to the electron and the fast part of the ion current and a longer tail, up to 200 ns, due to the slow part of the ion current. However, the relative amplitude is comparable, which indicates that the fast electron signal was highly suppressed because of insufficient rise speed of the amplifier. With the 50 microns gap the electron and ion signals overlap within 80 ns, but the fast component is still weaker than expected.

Using a current-sensitive preamplifier with a faster rise time (1 ns) the result is spectacular (Fig. 5) : the fast electron signal is much steeper (rise about 1 ns), still dominated by the electronics speed. But, the fast signal is now 10 times higher than the ion tail.

In the following sections we present experimental results obtained in two particle beams at CERN. In the first test (PS beam), charge preamplifiers (Gassiplex) have been used, providing a large detection plateau, while in the second run (SPS intense beam) where we used MQS104A chips the result was good but the efficiency plateau rather marginal, as predicted by the ballistic deficit observed in Fig. 4.

### 3 Beam tests at moderate particle flux

#### 3.1 Set-up

Our first tests of Micromegas were done with a gas filling of Argon-Isobutane [2]. We pursued with a more standard Argon-DME mixture. The amplification gap was  $100 \mu\text{m}$ .

The Micromegas detectors were on a platform between two drift chambers 3 m apart, giving two co-ordinate accuracy of  $150 \mu\text{m}$ . An event was triggered by a coincidence between upstream and downstream scintillation counters, defining a beam area of  $2 \text{ cm}^2$  in a CERN PS test beam (T9) of 10 GeV/c negative pions, diverging by 2 mrd horizontally and 1 mrd vertically.

Tests were made first with a doublet of Micromegas, with adjacent rear planes against each other, thus putting the detecting planes (middle of drift gap) at a distance of 9 mm. With this set-up we tested the characteristics of Micromegas with respect to the amplification gain and to different mixtures of Argon-DME.

Then a Micromegas chamber which can turn around an horizontal axis (along the strip direction), was placed in the middle of the platform, sandwiched by two Micromegas doublets 25 cm apart. Rotating the Micromegas in the middle of this set-up and using the two doublets as a telescope, we measured the dependence of the spatial resolution with respect to the track angle.

All the detectors Micromegas had an active surface of  $15 \times 15 \text{ cm}^2$ , but only the central part of the strips was electronically equipped (96 strips per plane).

The strip signals were collected on an ADC with the multiplexed electronics Gassiplex [3]. Three chips of 16 charge preamplifiers were connected in serial on each side of the detector. So 48 signals of one over two strip were multiplexed in time on one output to be read out in the ADC. On each strip, we measured an Equivalent Noise Charge (ENC) of 1500 electrons.

#### 3.2 Analysis

As a preliminary feature, we point out that the amplification gain deduced from the collected charge on strips is 7 times lower than the gain measured in laboratory with the signal induced on the mesh by a  $Fe^{55}$  source (Fig. 6). The biggest part of the strip signal loss was explained a posteriori in laboratory, by a bad timing in the peaking time of Gassiplex which was set at  $1 \mu\text{s}$  instead of 400 ns, and by a loss in the 30 m cables. Nevertheless the two exponential

slopes of the gain versus the mesh potential are in good agreement, which means that Micromegas was working as expected.

A second remark concerns the choice of the threshold in the search of clusters. This choice is a compromise between a low threshold to insure a good efficiency and a higher one to reduce the number of noisy strips. On Fig. 7 it is clear that a reasonable cut is between 3 and 6 (in pedestal standard deviation units). For most of the following we have chosen a threshold at 3. Note that the noise at high cut doesn't drop to zero. This is due to remaining double tracks encoded by the Gassiplex electronics which has a long integration time of the order of 600 ns.

Another interesting feature is the good uniformity of the Micromegas response (Fig. 8), except in the pillar zones. The spacers (200  $\mu\text{m}$  diameter), which maintain the 100  $\mu\text{m}$  gap between the micromesh and the strips, are disposed every 2 mm, aligned on every 6th strip. On Fig. 8 we see the effect of the spacers. They induce a loss on signal of 7% on the strips (modulo 6) where they lay, as expected from the geometrical acceptance. The resulting efficiency loss is negligible, less than 1%.

### *3.3 Mesh potential dependence*

#### *3.3.1 Efficiency*

In the first data, the drift voltage is fixed at 850 Volts. With the gas mixture of 90% Argon and 10% DME, we observe an efficiency plateau of 25 Volts (Fig. 9) at a level of 99%. Beyond a gain of 35000 reached at 395 Volts, we observed an increase in the frequency of sparks. Although they are not destructive, neither for the chamber nor the electronics, we stop at this level. As mentioned previously, we have lost a factor 7 in the signal. So in fact, the length of the plateau should be 50 Volts larger.

A typical distribution of the collected charge is shown in the enclosed Fig. 9. The ratio of the charge of the cluster (S) to the noise (N) of a strip is 40 at the peak for 395 Volts. This shape looks like a Landau distribution as expected by the fluctuation in the number of electrons created in the conversion gap.

#### *3.3.2 Cluster size*

The size of a cluster on a track is defined as the number of adjacent strips with collected charge above 3 ENC, the cut we used in the analysis. The cluster size grows smoothly with the mesh potential (Fig. 10) from 2 at the beginning of the efficiency plateau to 2.7 at the end. It means the strip pitch



is well adapted to these operating conditions.

### *3.3.3 Spatial resolution*

The spatial resolution is determined with the doublet of detectors where the two points on a track are so close that the multiple scattering is negligible. The difference between the two centroids, corrected from the track angle given by the drift chambers, has a gaussian distribution (enclosed Fig. 11). Assuming the two Micromegas have the same resolution, the standard deviation of this distribution, divided by  $\sqrt{2}$ , gives the resolution. The spatial resolution, of the order of  $65 \mu m$ , is independent of the gain of the chamber (Fig. 11). Our Monte-Carlo shows that the resolution is mainly due to the transverse diffusion of the gas. The agreement with the data is obtained with a transverse diffusion of  $200 \mu m$  in the 3 mm drift gap.

### *3.4 Gas mixture dependence*

We have worked with Argon mixed with DME at concentration of 7%, 10% and 15% at a constant gain of 2700, measured on strips, where the efficiency is 99%. We observe a decrease in the cluster size with the DME concentration (Fig. 12a) which shows the effect of a decrease in the transverse diffusion. The cluster size decreases from 2.6 at 7% to 2.1 at 15% DME, with an improvement in position resolution (Fig. 12b) reaching  $55 \mu m$ .

### *3.5 Track angle dependence*

With the second set-up we took data with the rotating chamber in order to estimate the effect on the spatial resolution of the angle of the track on the detector plane.

We came back to the gas mixture of 90% Argon with 10% DME. The drift voltage was fixed at 1000 Volts and the mesh voltage at 370 Volts which corresponds to the beginning of the plateau efficiency. During this run we could not solve a tiny leakage in the gas circulation. As a consequence the efficiency is not so good as previously, limited at 95%, but stays at this level for any track angle up to 35 degrees.

The spatial resolution of the rotating Micromegas is determined with the two Micromegas doublets used as telescope. The interpolated point is obtained from the doublet points with a precision of  $50 \mu m$ . Convoluted with the  $18 \mu m$  due to multiple scattering, we get the error of the expected point of the track

in the rotating detector. The standard deviation of the difference between the centroid of the cluster and the interpolated point gives the spatial resolution, after deconvolution of the expected error.

The Fig. 13 shows a strong dependence of the position resolution with the track angle. It fits well with a convolution of two terms: a constant term,  $71 \mu\text{m}$ , which corresponds to the resolution at normal incidence; a second term,  $195 \mu\text{m}$  per mm, proportional to the length of the piece of track through the conversion gap projected on the detector plane, which describes the degradation of the spatial resolution.

#### 4 Gas optimization

In order to improve spatial resolution we have to use gas mixtures of smaller transverse diffusion and smaller strips. A study has been undertaken to optimize the primary ionization, drift and diffusion of the electrons and the gas amplification process. The last three parameters are closely linked to the nature of the gas mixture. In such a detector, designed for high rates, it is important to find a gas mixture which allows a maximum gain around  $10^5$ : although the gain range of operation will be between  $10^3$  and  $10^4$ , a higher maximum gain gives the necessary margin, to prevent sparks in the detector. Moreover, the gas mixture must have a drift velocity as high as possible to improve the time resolution.

Several gas mixtures have been tested and detailed results will be published in a coming paper. We have found a very satisfactory new gas filling : Argon + Cyclohexane with a possible adjunction of  $\text{CF}_4$ .

Bubbling Argon through Cyclohexane at controlled temperature we can vary the proportion of vapors which is 8% at  $15^\circ\text{C}$ . At a pressure of 1 bar we can see (Fig. 14) the dependence of the maximum gain which can be reached as a function of Cyclohexane concentration in Argon, with a  $50 \mu\text{m}$  gap. The optimum is around 4% and permits a maximum gain of  $3.5 \times 10^5$ . The Fig. 15 shows the efficiency versus the voltage applied on the micromesh for two different conversion gaps obtained with 10 GeV pions. The plateau is quite large, 50 Volts at 340 Volts, with a 3 mm conversion gap. The efficiency of the 1 mm conversion gap reaches 96%, with a narrower plateau of 25 Volts, but it is expected to be larger for the next scheduled beam-tests, with improved electronics.

The admixture of various proportions of  $\text{CF}_4$  has a strong influence on both electron drift velocity and electron diffusion in the conversion gap: electron velocity increases and the diffusion coefficient decreases. With 20% of  $\text{CF}_4$

admixture the maximum gain is still high,  $1.5 \times 10^5$ . The most promising mixture is pure  $\text{CF}_4$  and a small proportion of Cyclohexane. As shown in Fig. 16, the maximum gain achieved with 7% Cyclohexane is high,  $6 \times 10^4$ , when the detector is irradiated with 5.9 keV X-rays, at low flux. It is still significant,  $10^4$ , at high flux,  $5 \times 10^5 \text{ Hz} / \text{mm}^2$ , in a 8 KeV X-ray environment.

## 5 Micromegas in a Fast Rate Environment

We have already observed [2] that the gain of the detector do not saturate up to breakdown. The maximum achievable gain, however, decreases with the flux (Fig. 17), but still higher than 1000 at flux of  $10^7 \text{ Hz} / \text{mm}^2$ . Which means that, with a good electronics (noise of the order of 1000 electrons) Micromegas can operate with full efficiency at so high fluxes.

We have pursued our study with the goal of adapting Micromegas to experiments projected in the near future, one of them being COMPASS [4]. In the very-forward region of the experiment it requires chambers operating at rates higher than those foreseen at LHC :  $10^6 \text{ Hz} / \text{cm}^2$ . To deal with such an environment we have to optimize the time resolution of the detector as well as some geometrical parameters. The depth of the amplification gap controls the occupation time of the positive ions. The depth of the drift gap determines the signal width due to the drifting electrons. The limit is set by the need of an efficiency close to unity.

In view of the large number of channels foreseen at COMPASS (several tens of thousands), a digital read out was tested. The time of both the leading and the trailing edges of the signal was recorded with multihit TDC's. Thus the width of each signal is known and allows to reject the noise which has a very small width. The width is also used to improve the spatial resolution since it is correlated with the charge.

Fig. 18 shows the efficiency as a function of the applied voltage in the amplification gap. It is difficult to reach a plateau. As already pointed out this electronics is too slow for the signal induced by the electrons in the avalanche (1ns) and too fast for the signal induced by the ion motion, which results in a reduced gain. To obtain a good efficiency the electronic time constant should be increased to 30 ns and the electronic noise decreased to about 1000 electrons.

We have measured the time jitter of the electronic signal with respect to the trigger time. With pure Argon + Cyclohexane mixture the time resolution is 20 ns (RMS). Adding 30% of  $\text{CF}_4$  improves the time resolution to about 5 ns (RMS), but reduces the efficiency.

## 6 Micromegas in a magnetic field environment

The performances of Micromegas have also been studied in a magnetic field up to 1.3 Tesla. We have installed two Micromegas chambers in the experimental set-up of TOSCA [5], prototype of a spectrometer inside a dipole magnet. The test was performed in the CERN-PS pions beam T9. The two Micromegas chambers were filled with 90% of Argon and 10% of Isobutane. Silicon strips detectors have been used to reconstruct with high resolution the extrapolated point of the track in Micromegas.

Preliminary results indicate that the amplification gain is not affected by the magnetic field. The Lorentz angle is found at the expected value, 15 degrees at 1 Tesla. The resolution with the gas used is  $80 \mu\text{m}$  for normal incident tracks without magnetic field. At 1 Tesla, it grows up to  $110 \mu\text{m}$  due to the Lorentz angle. Turning the detector to compensate this angle, the resolution is restored to about  $80 \mu\text{m}$ . So, if there is a degradation due to the magnetic field, it is small compared to  $80 \mu\text{m}$ .

## 7 Outlook

To optimize the properties of the detector, we have to pursue our study on different parameters : the gas, the geometry and the electronics.

Concerning the gas, we think that  $\text{CF}_4$  mixture is the most promising. It yields the highest drift velocity,  $2 \times 10^7 \text{cm/s}$ , allowing excellent time properties and its diffusion coefficient is expected to be as low as 70 microns per 1 cm path [6].

The use of  $\text{CF}_4$  mixture constitutes a key point to improve the spatial resolution. As it has been shown, the obtained spatial resolution ( $60 \mu\text{m}$  with Argon-DME mixture) was limited by the transverse electron diffusion in the conversion gap. By using  $\text{CF}_4$  mixtures the diffusion coefficient can decrease by a factor of three. At the same time the number of primary electrons, produced by the incident particle in the drift gap, is 3-4 times higher in this mixture, which improves the accuracy of the charge interpolation between anode strips.

The decrease of the diffusion coefficient must, however, be combined with a decrease of the anode pitch in order to keep the strip multiplicity, per incident particle, at the order of 2, which is the optimal value for efficient charge interpolation. Monte Carlo simulations show that spatial resolution of about 10 microns is within reach with anode pitch of 100 microns.

Using  $\text{CF}_4$  as carrier gas, one can further reduce the conversion gap below 1 mm and still keep full efficiency of the detector. Such a small gap will limit the degradation of the spatial resolution due to inclined tracks or the presence of strong magnetic field and will improve the time resolution. The time resolution (5 ns) obtained is limited by the preamplifier rise time. It can be improved by using faster preamplifiers. Our objective is to achieve, in the near future, time resolution of 1 ns.

The way is open to operate high resolution detectors in the GHz region able to cope with intense radiation environments.

## 8 Conclusions

Further steps have been made in the development of a very-high rate, high precision gaseous detector Micromegas. We have tested several  $15 \times 15 \text{ cm}^2$  detectors in intense particle beams. The results indicate a good behaviour of the detector. After a total of 3 month tests in hard radiation environment the detector was stable and reliable.

Our major results are :

- Detector can operate at a gain of  $10^4$  at rates of  $10^6 \text{ Hz} / \text{mm}^2$ , without any damage of the detector or electronics. No sign of aging of the detector has been observed for various gas mixtures.
- Using a charge preamplifier, at moderate fluxes, full efficiency with large plateau is obtained with several gas mixtures. With a conversion gap reduced to 1 mm the efficiency was 96%. Position resolution of 60 microns was measured with an Argon and DME gas mixture. The limitation was due to the diffusion of primary electrons in the gas.
- A time resolution of 5 ns (RMS) was achieved when working with 30% of  $\text{CF}_4$ . With adequate fast preamplifiers, signals with 1ns rise time have been obtained reflecting the fast movement of the electrons during the avalanche development.
- A magnetic field environment, up to 1.3 Tesla, has no effect on the amplification gain of the detector.

Finally all the tests indicate that the operation of the detector depends on many parameters, which have to be optimized for any particular purpose. A detector with optimized pitch, electronics and gas mixture is under construction to explore the ultimate spatial and time resolution. It can be of high importance not only for the tracking in high energy experiments but also for

the vertexing (impact parameter). We are also studying a new pixel detector to be used close to the interaction region at the highest LHC luminosity.

## Acknowledgements

We thank Ph. Abbon, Ph. Briet, B. Cahan, R. Durand, R. Frei, A. Giganon, D. Jourde, J.-P. Robert for chamber and electronics construction, C. Mazur and R. Veenhof for their help.

## 9 Figure captions

Fig. 1. *Micromegas electric field map*

Fig. 2. *Expected gain as a function of the amplification gap at various potentials.*

Fig. 3. *Signal given by a charge preamplifier, for 50 and 100  $\mu\text{m}$  amplification gap.*

Fig. 4. *Signal given by the MQS104A chip, for 50  $\mu\text{m}$  (top) and 100  $\mu\text{m}$  (bottom) amplification gap.*

Fig. 5. *Signal given by a current preamplifier.*

Fig. 6. *Gain measured on mesh (in laboratory) and on strips (in beam) as a function of the mesh potential.*

Fig. 7. *Efficiency and fraction of noisy strips as a function of the strip noise threshold.*

Fig. 8. *Micromegas response on the strip which gives the highest signal in a cluster. Enclosed the mean response modulo 6 strips. Strips with spacer on are marked by a dot.*

Fig. 9. *Efficiency plateau. Enclosed the response distribution at 395 Volts.*

Fig. 10. *Cluster size as a function of the mesh potential. Enclosed the strip multiplicity distribution at 395 Volts.*

Fig. 11. *Spatial resolution as a function of the mesh potential. Enclosed the difference between the two centroids in the doublet at 395 Volts.*

Fig. 12. *Variation as a function of DME concentration of the a) cluster size b) spatial resolution.*

Fig. 13. *Spatial resolution as a function of the tangent of the track angle. The fit is the square root of the quadratic sum of two terms.*

Fig. 14. *Gain as a function of the amplification electric field for different Cyclohexane concentrations in Argon.*

Fig. 15. *Efficiency plateau for 3 and 1 mm conversion gap.*

Fig. 16. *Gain as a function of the amplification electric field with a gas mixture of different Cyclohexane concentrations in  $CF_4$ .*

Fig. 17. *Maximum gain as a function of 8 KeV X-rays flux.*

Fig. 18. *Efficiency as a function of the mesh potential measured with the MQS104A chip, for 100 and 50  $\mu m$  amplification gap.*

## References

- [1] Y. Giomataris, Ph. Rebourgeard, J.P. Robert, G. Charpak, NIM A376 [1996] p29.
- [2] G. Charpak et al., CERN LHC/97-08(EET), DAPNIA-97-05, to be published in NIM A.
- [3] J.C. Santiard et al., CERN-ECP/94-17, NIM A360 [1995].
- [4] CERN/SPSLC 96-14 SPLSLC/P297 and CERN/SPSLC 96-30 SPLSLC/P297 add.1.
- [5] Letter of Intent, A High Sensitivity Short Baseline Experiment to Search for  $\nu_\mu \rightarrow \nu_\tau$  Oscillation, CERN-SPSC/97-5.
- [6] S.F. Biagi, NIM A273 [1988] p533 and NIM A283 [1989] p716, MAGBOLTZ Source Code.

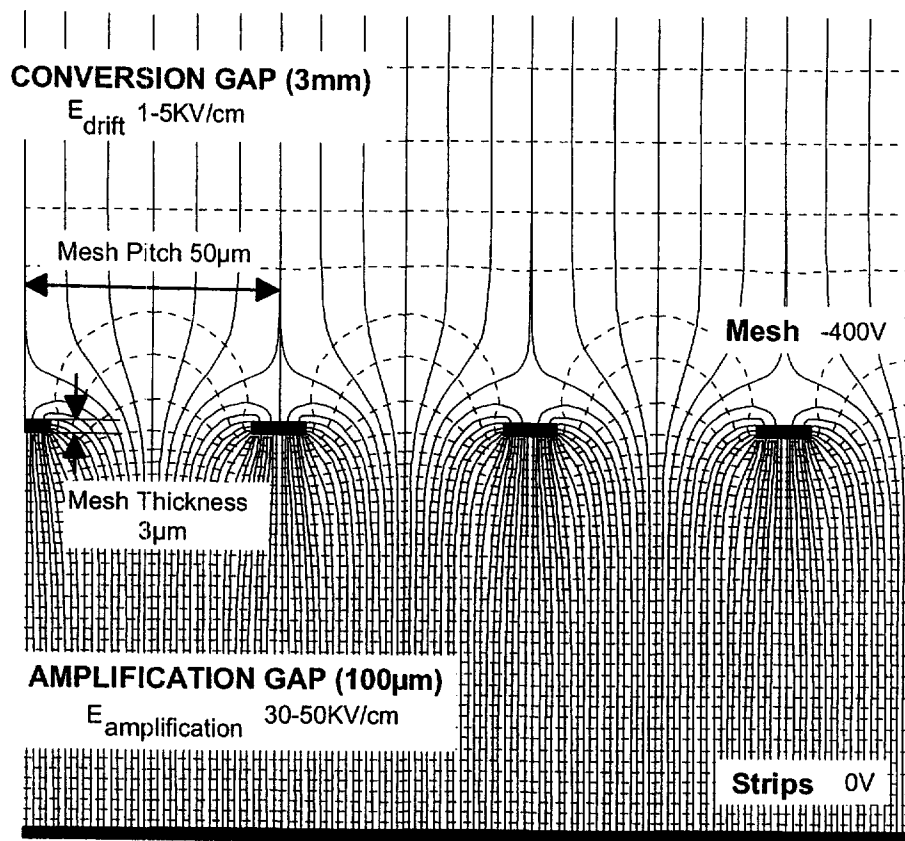


Fig. 1



Argon +5% DME

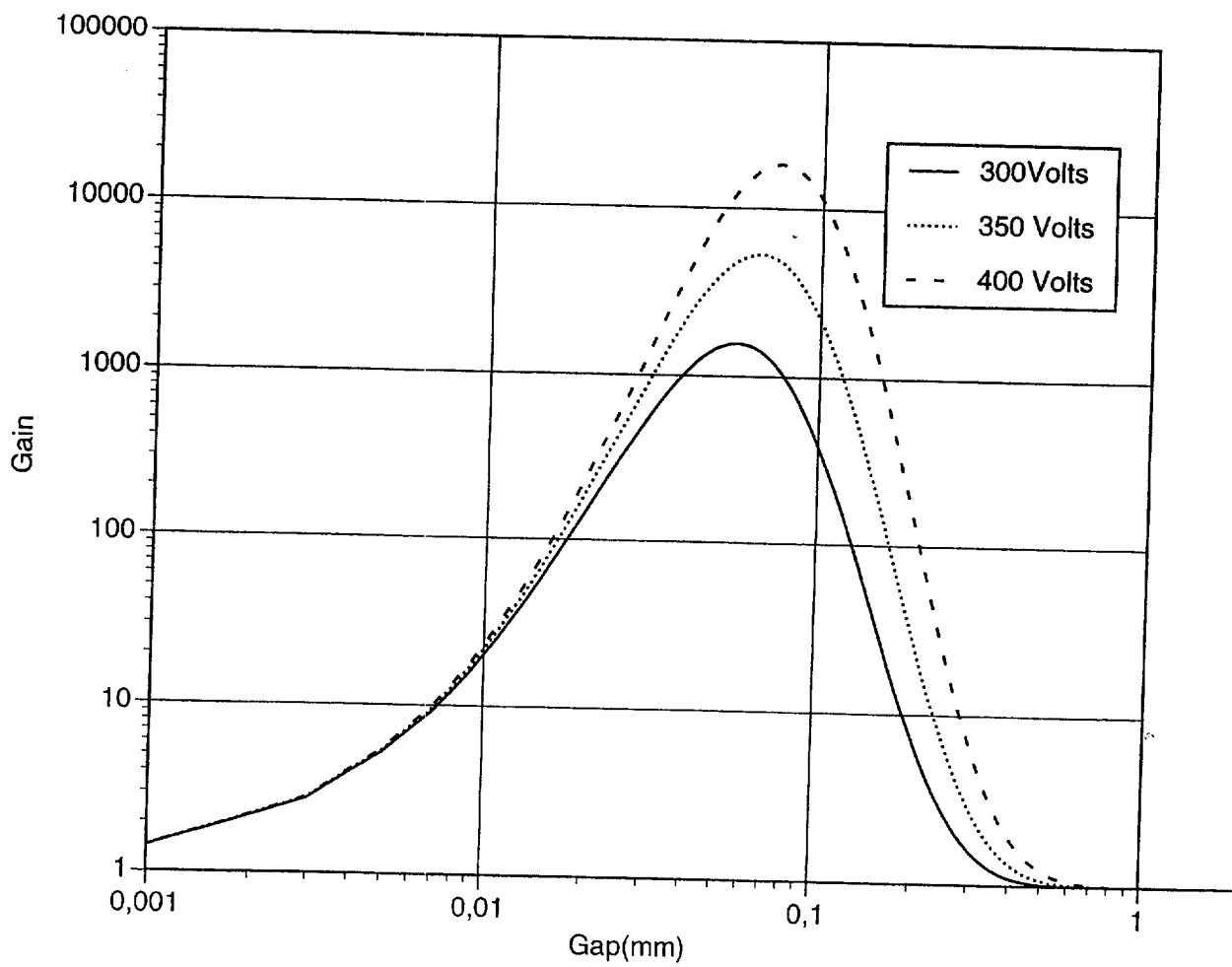


Fig. 2

Ar+10% Isobutane

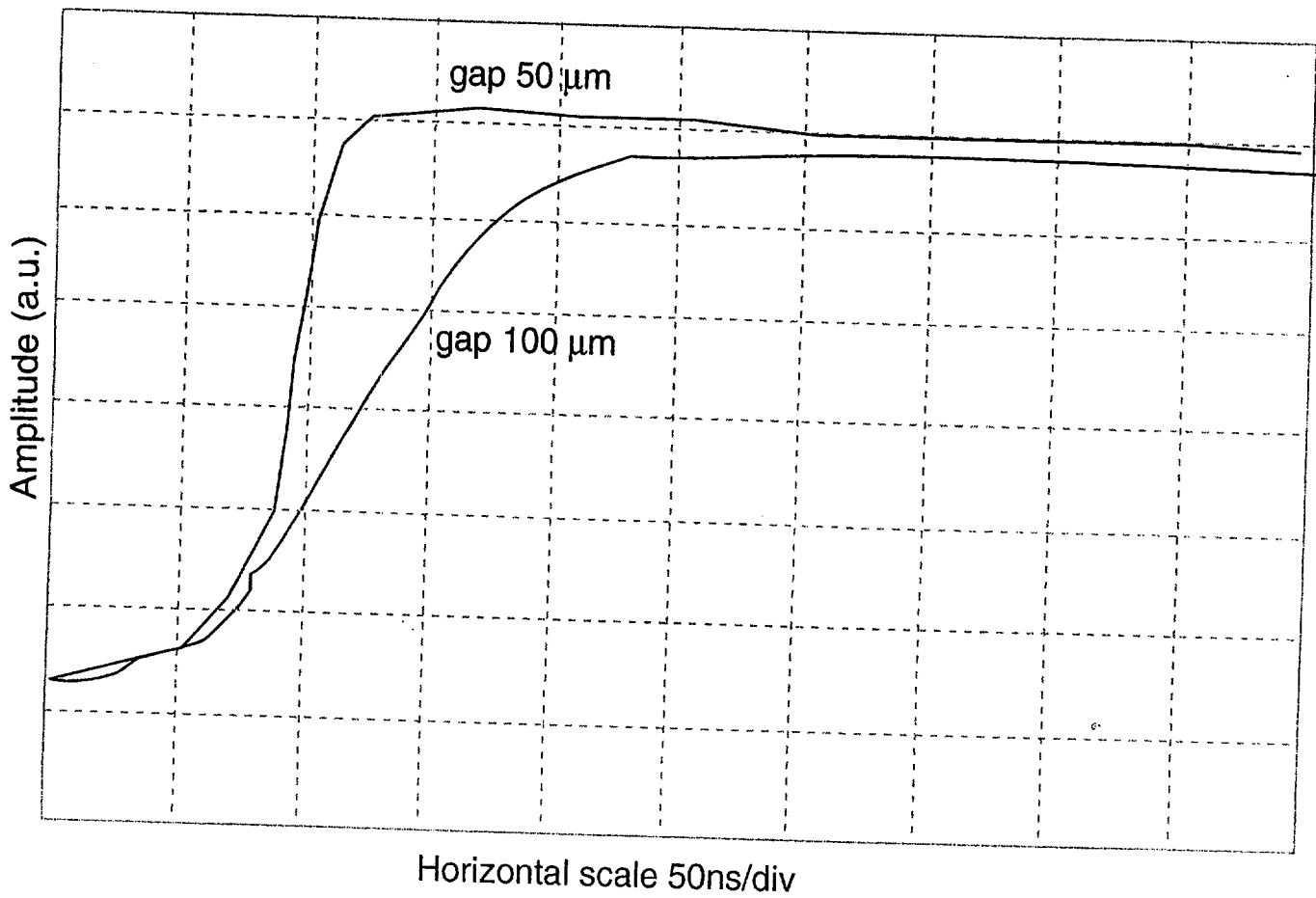


Fig. 3

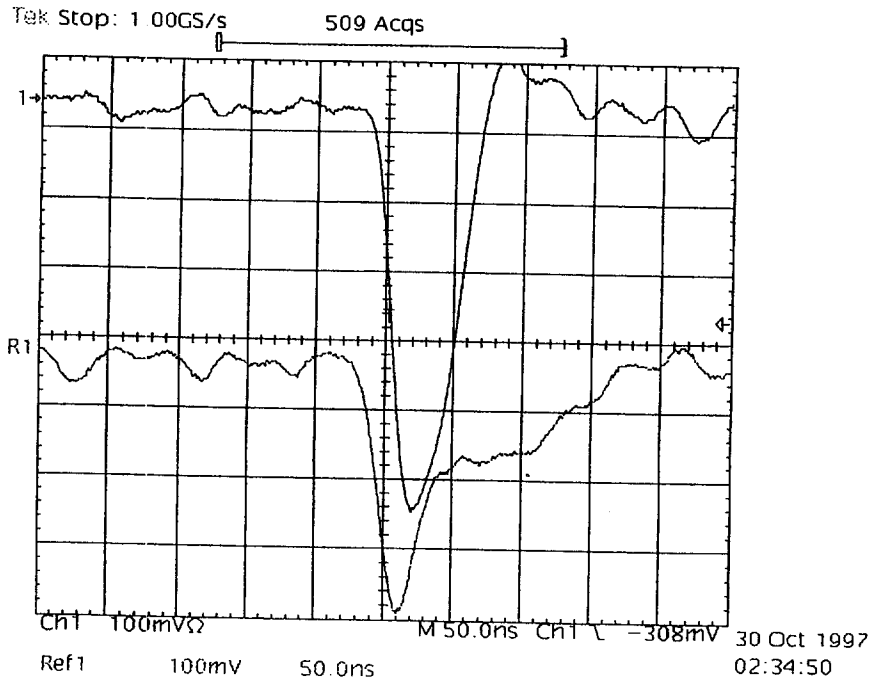


Fig. 4

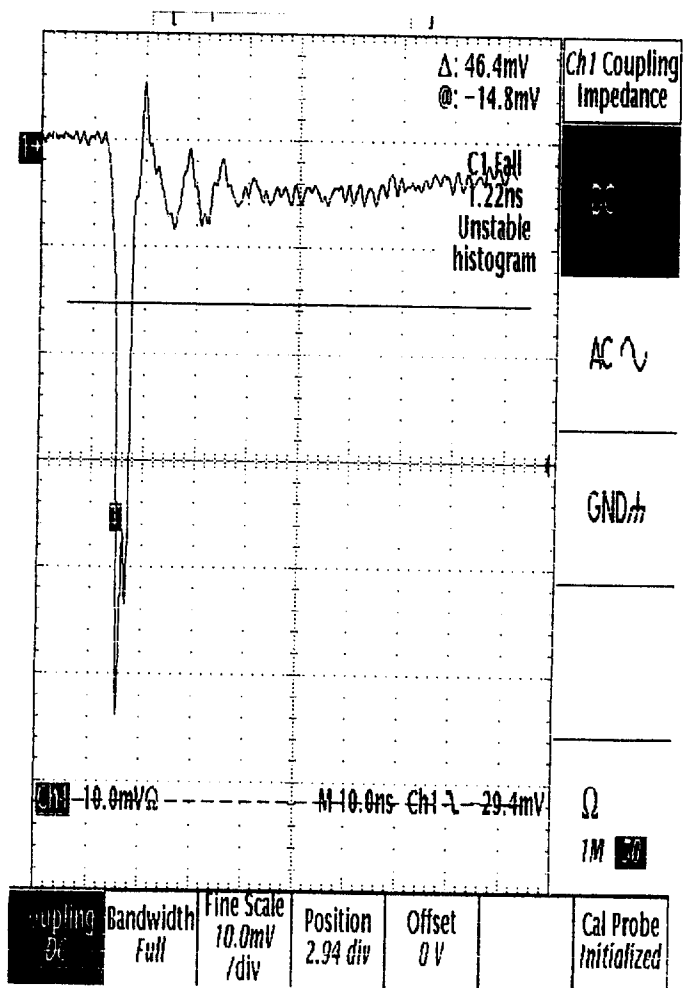


Fig. 5

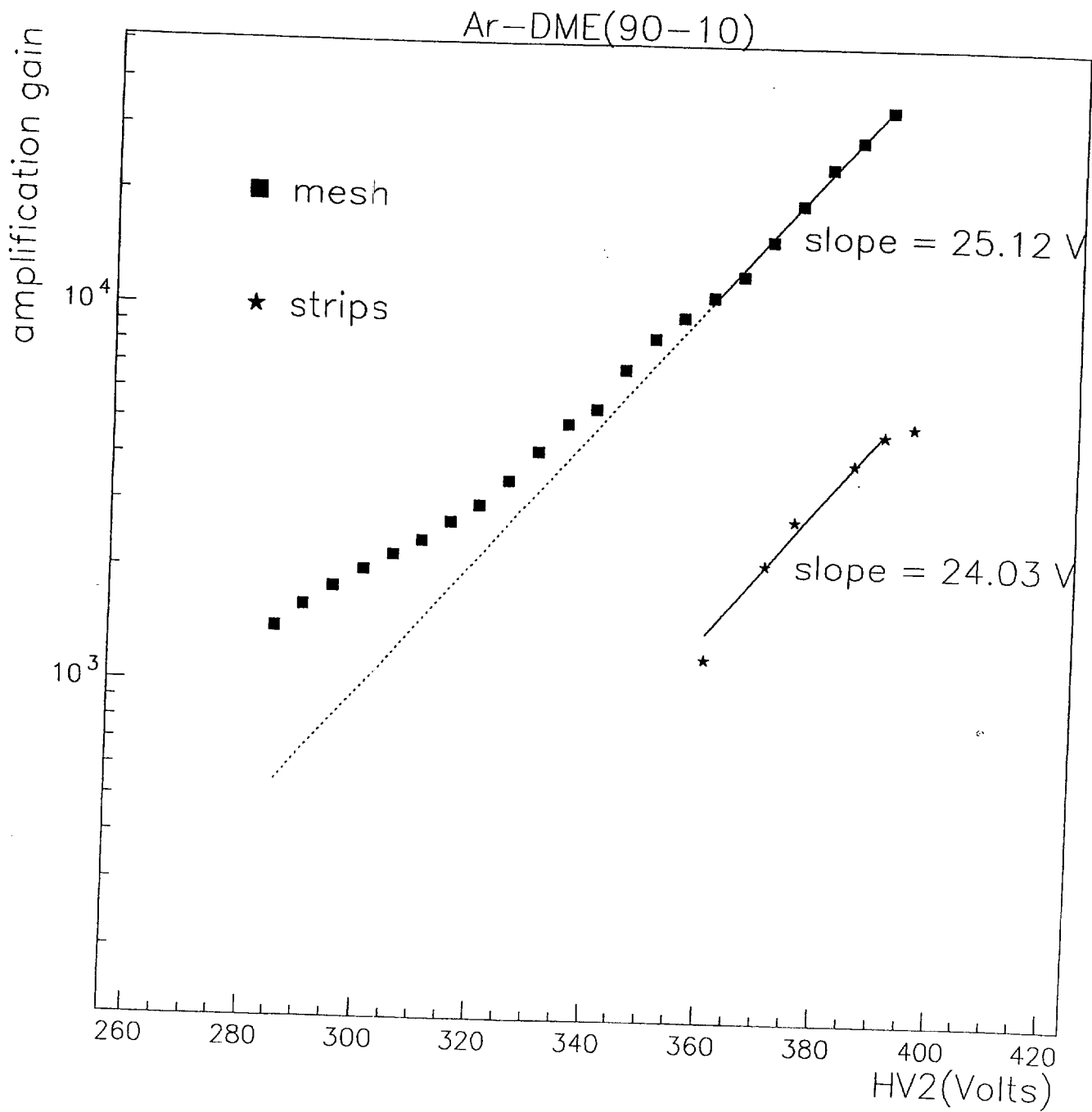


Fig. 6

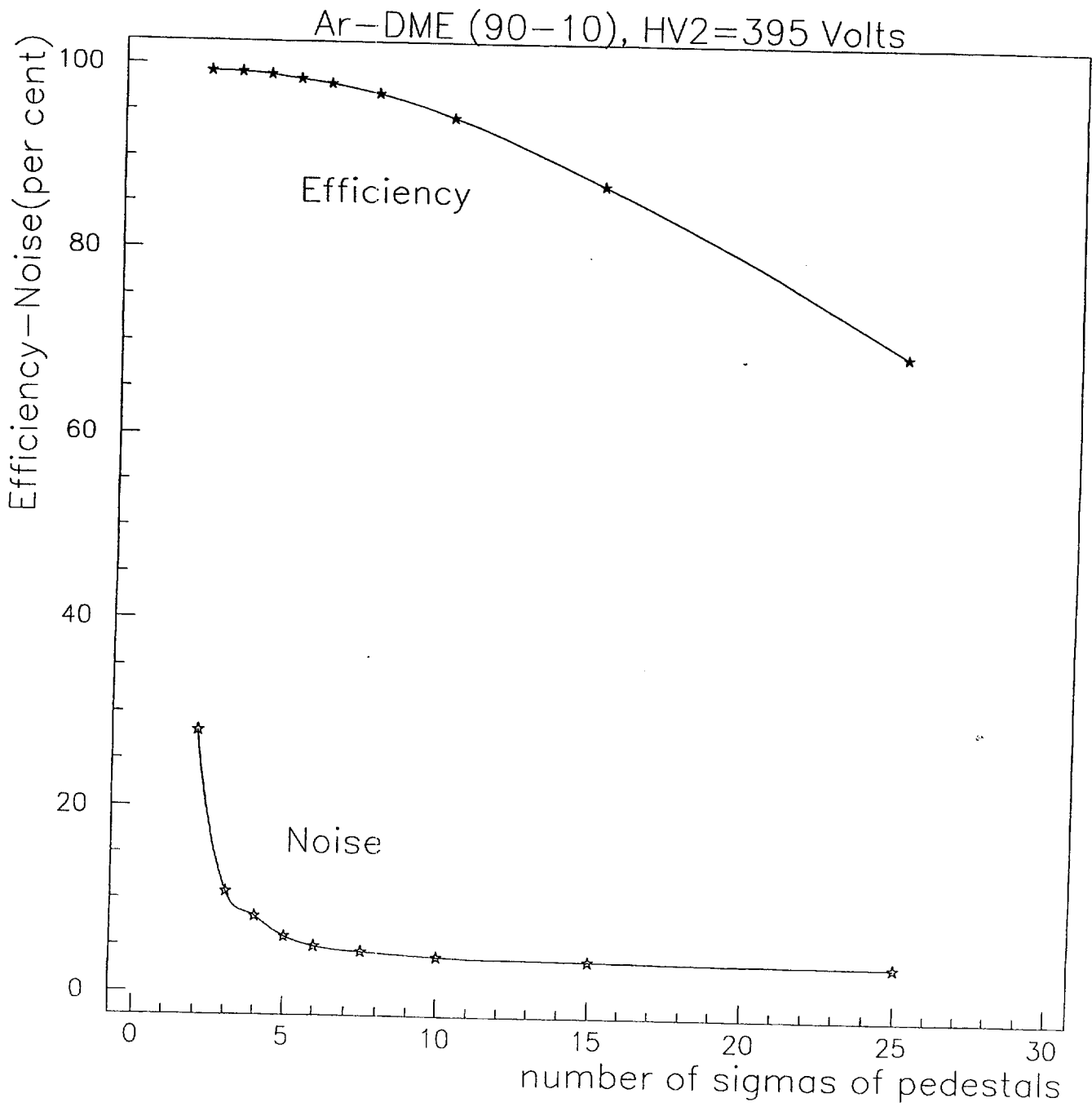


Fig. 7

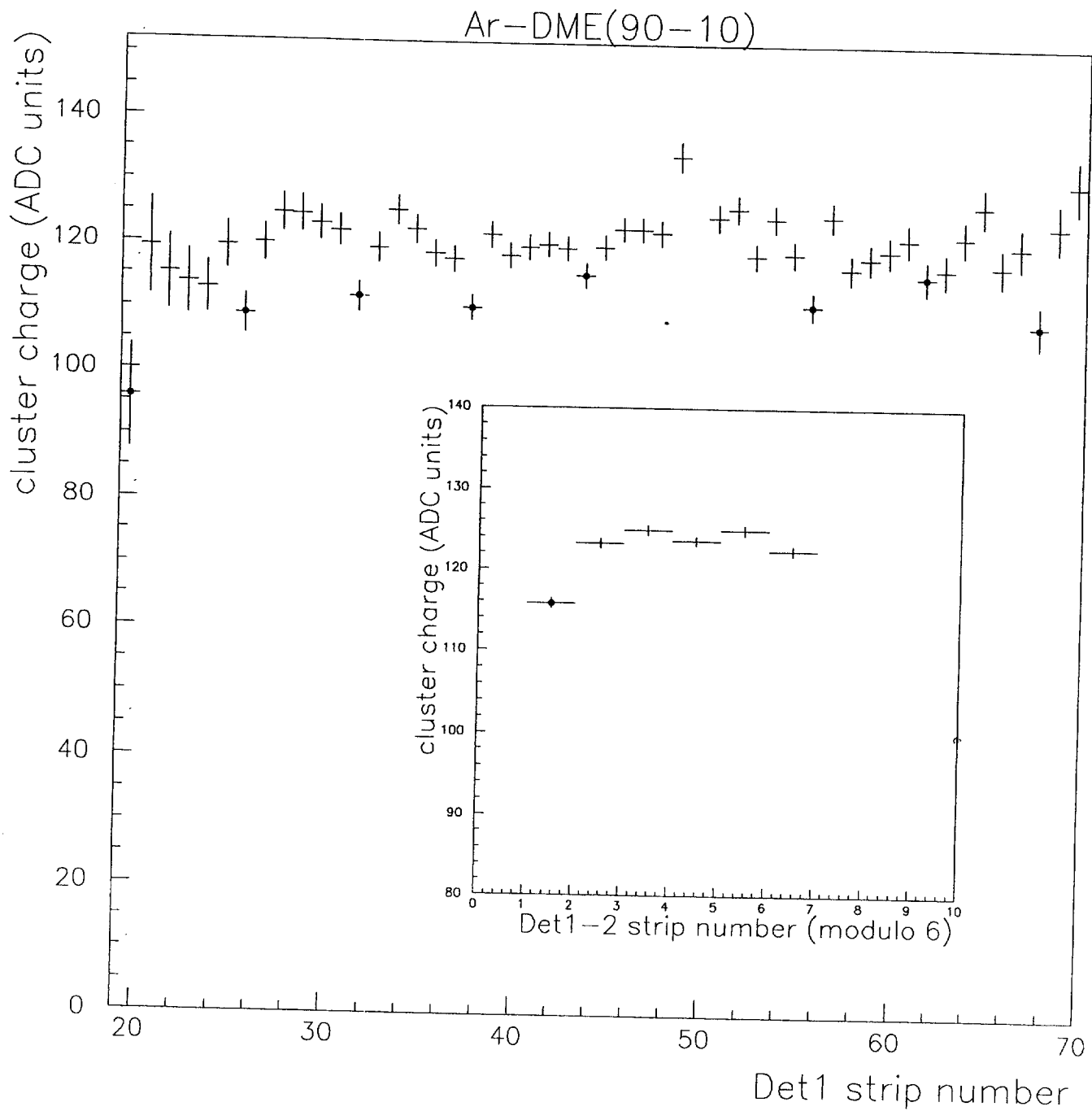


Fig. 8

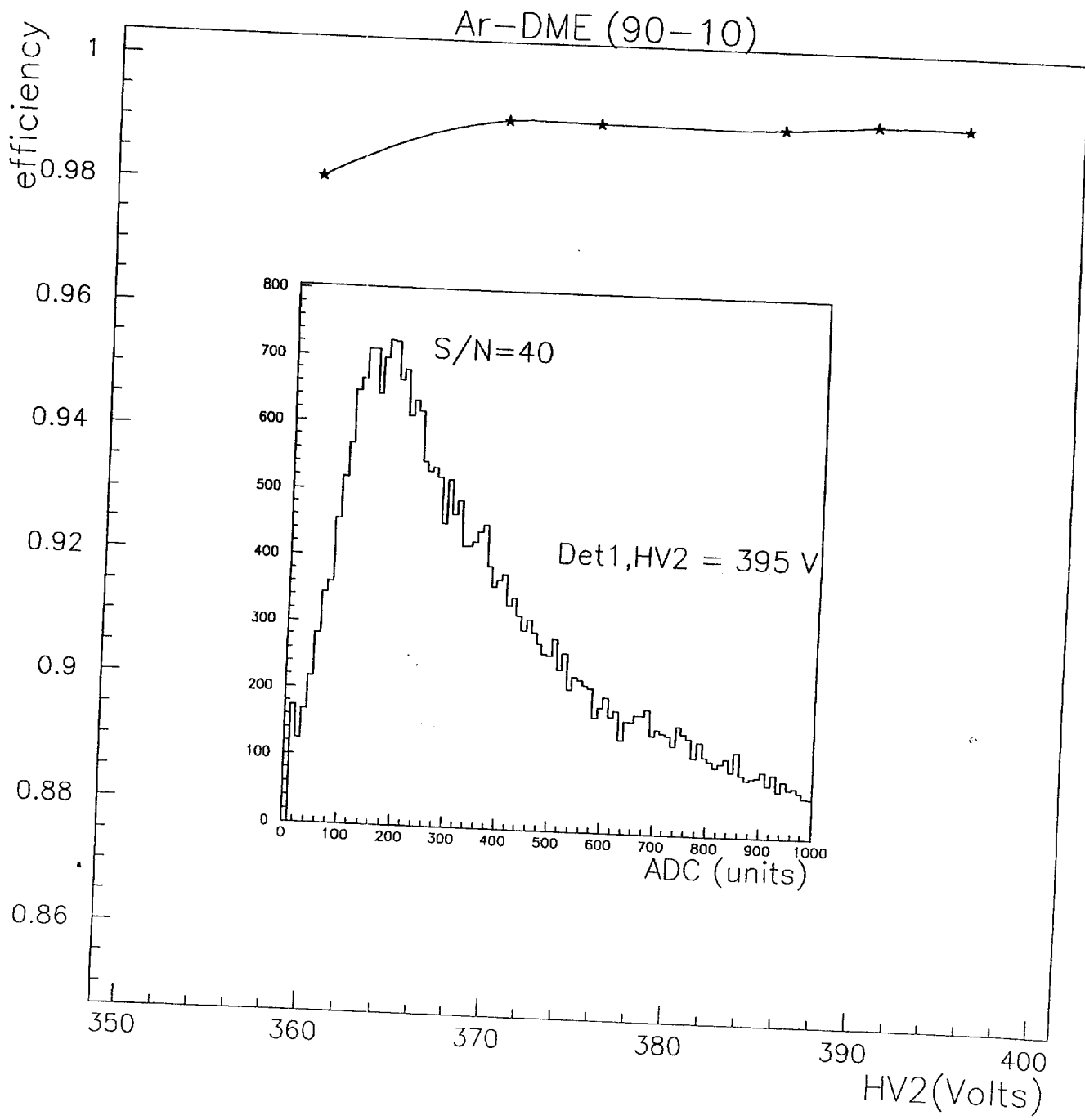


Fig. 9



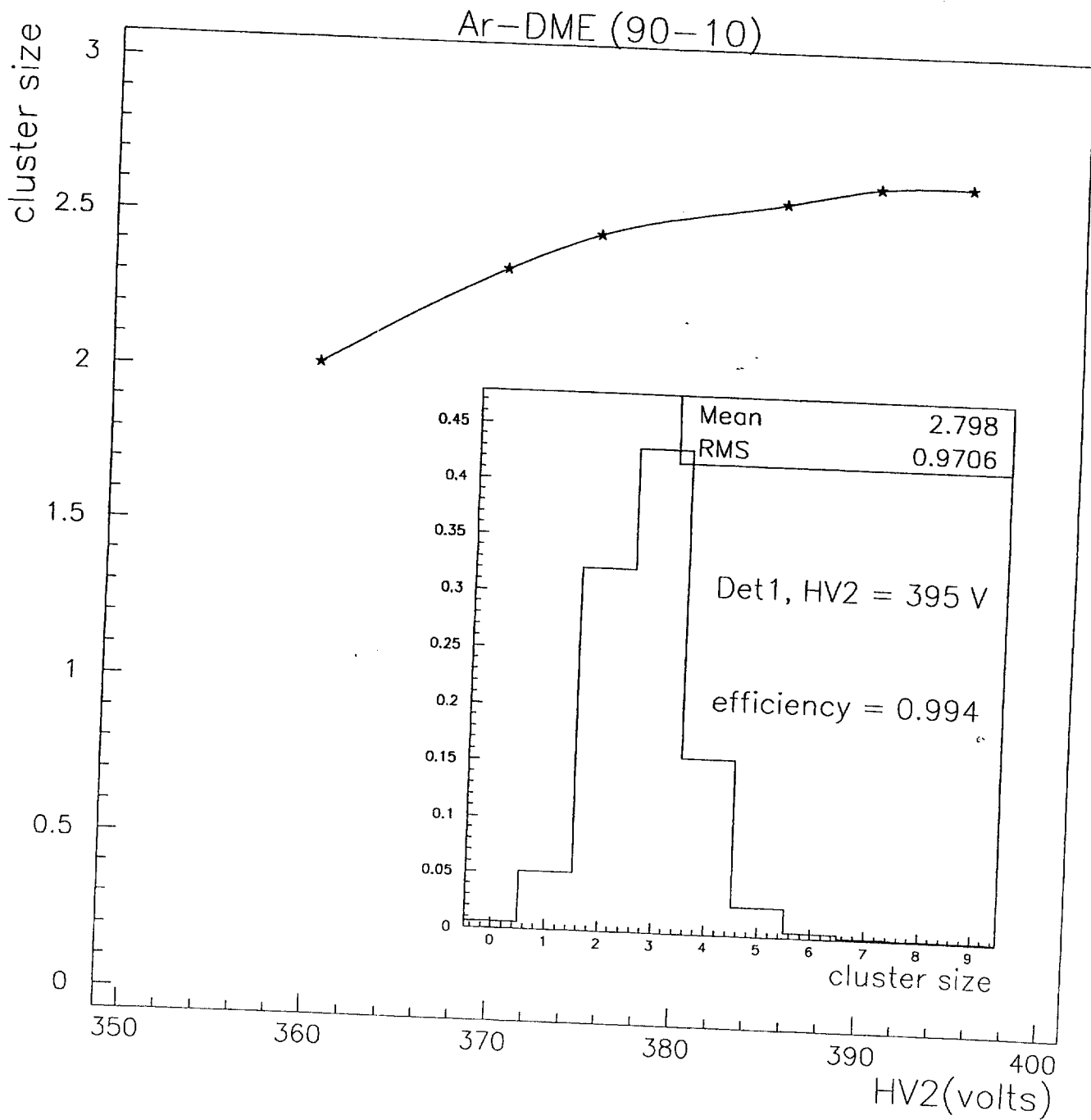


Fig. 10

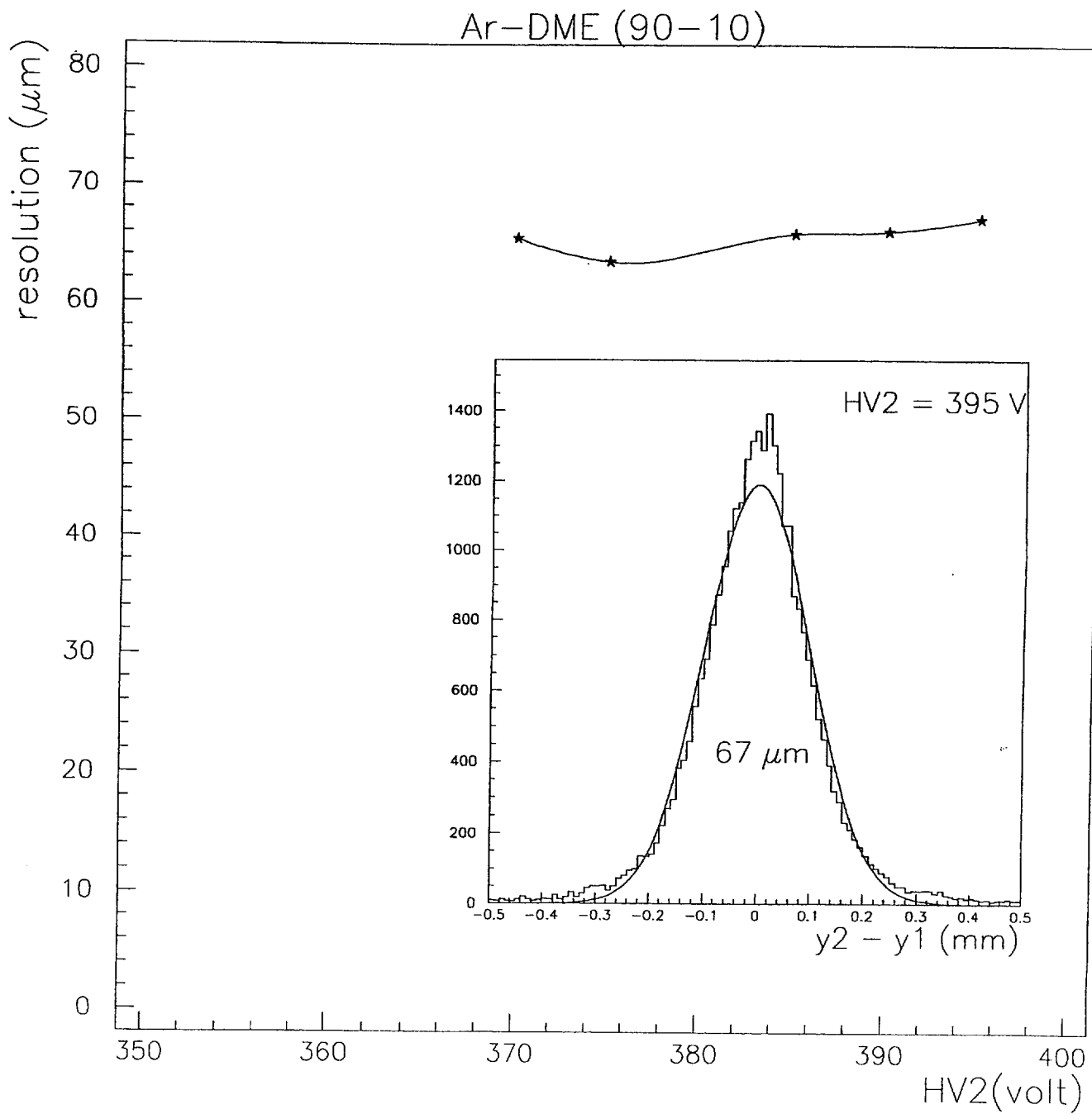


Fig. 11

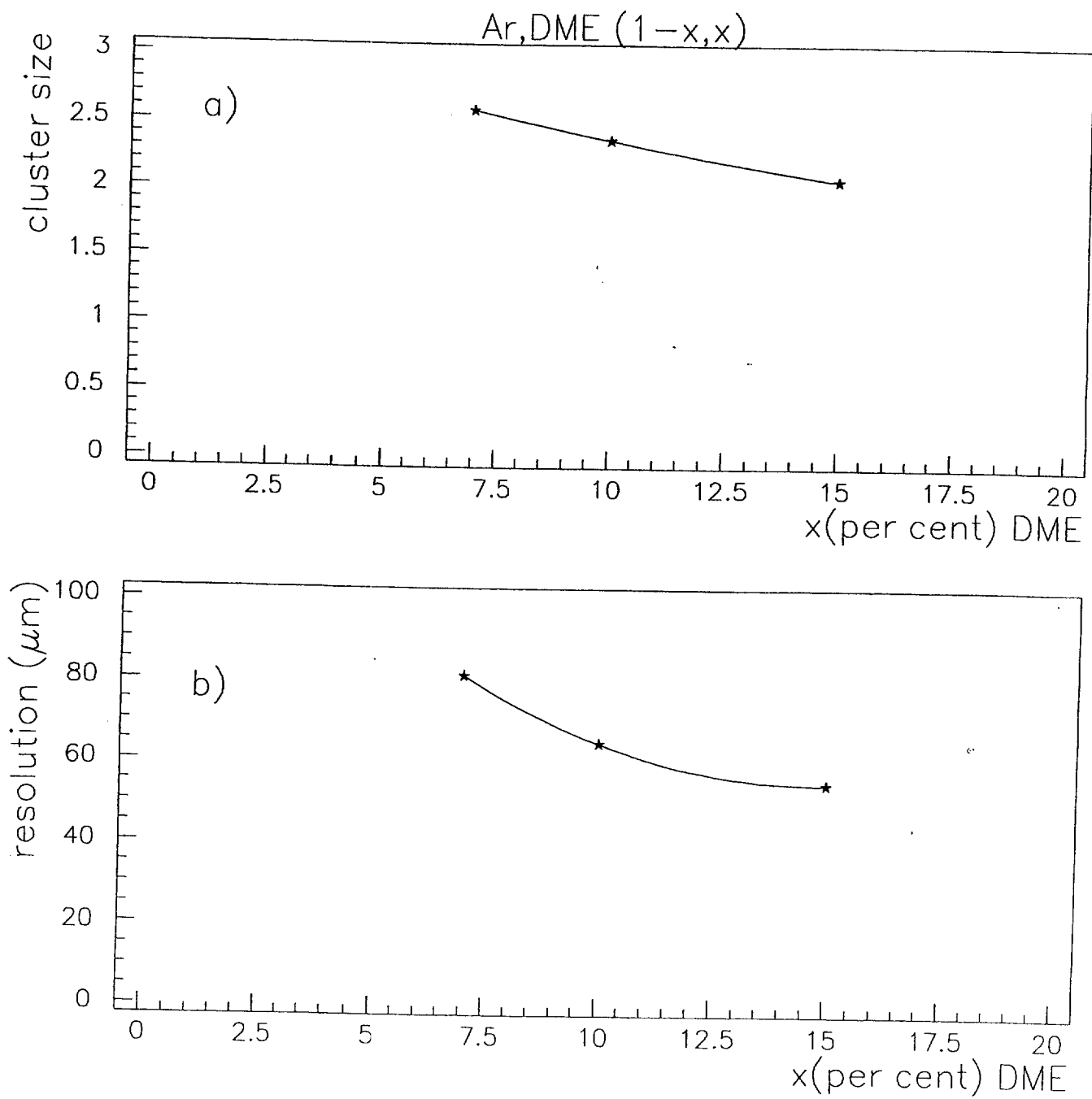


Fig. 12

Ar-DME (90-10)

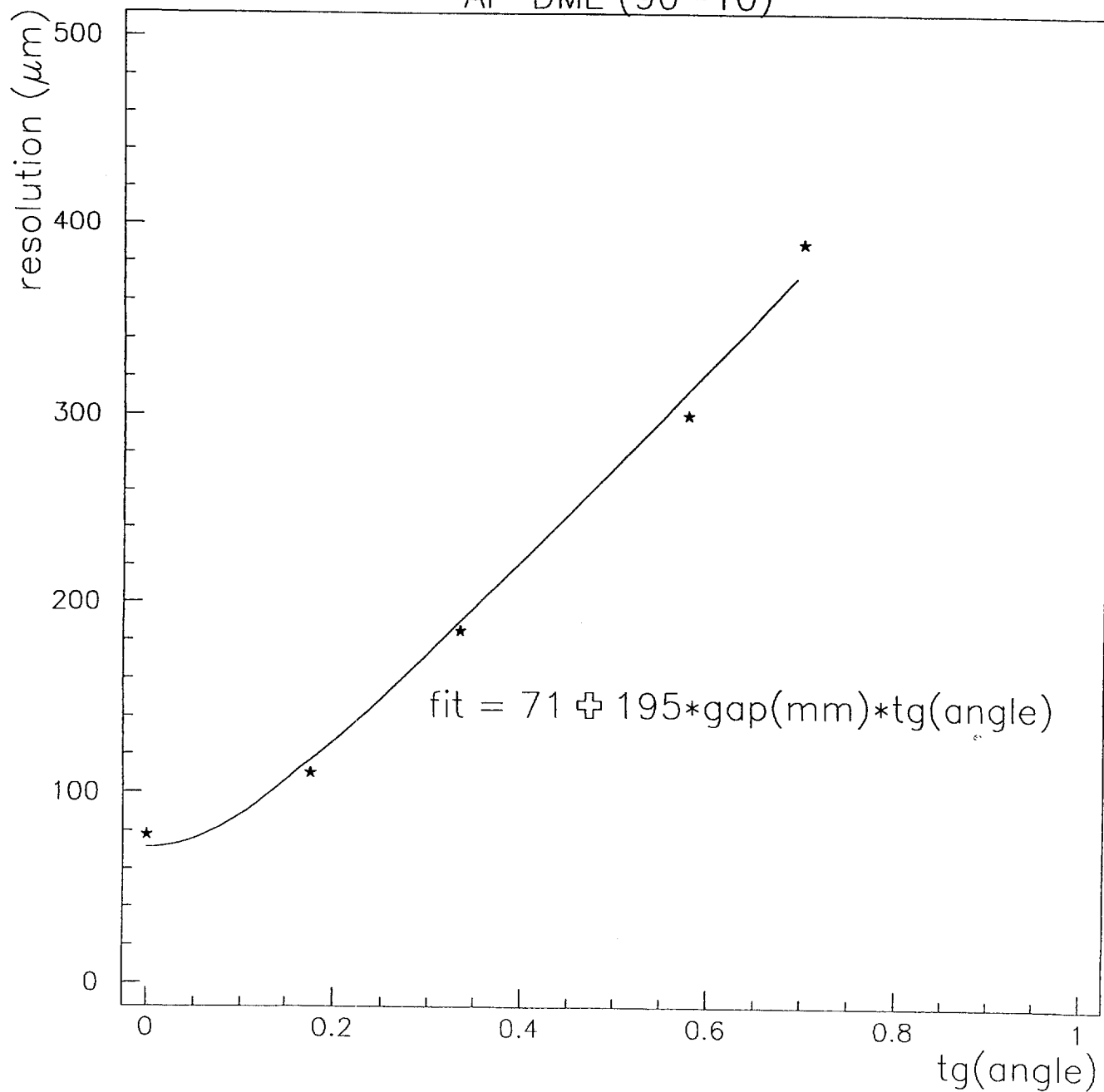


Fig. 13

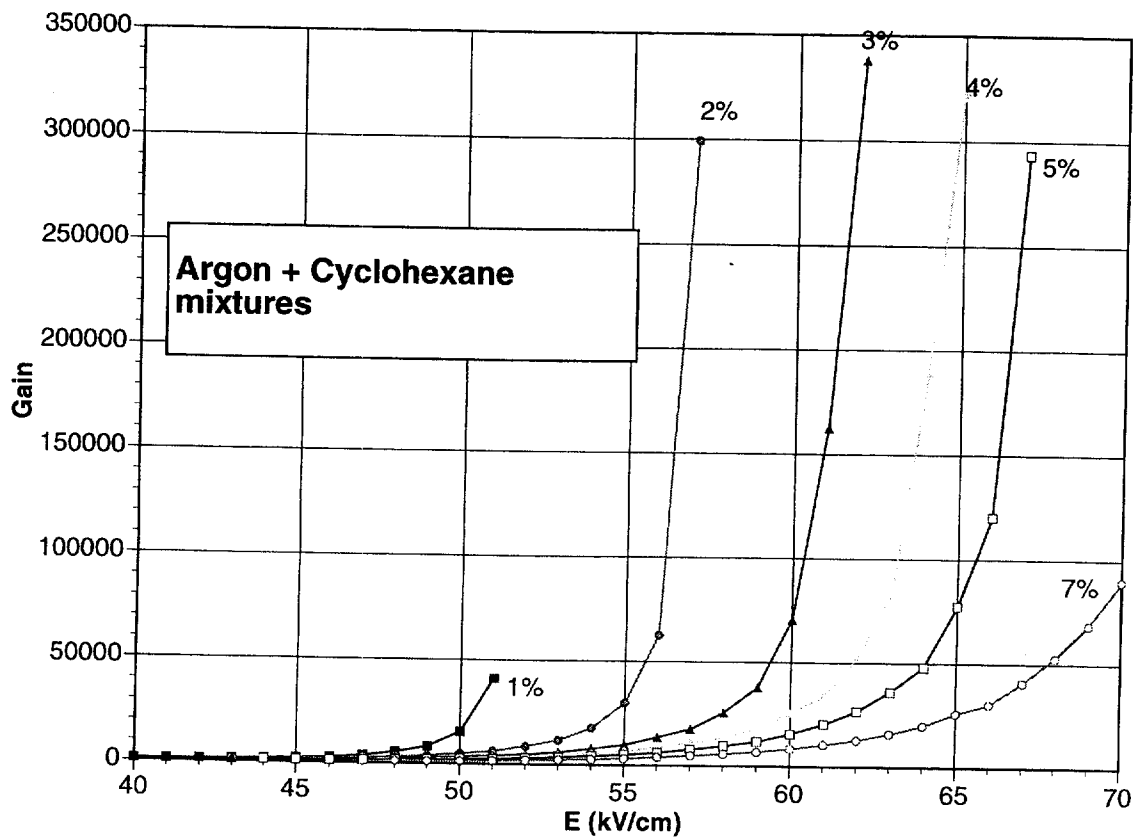


Fig. 14

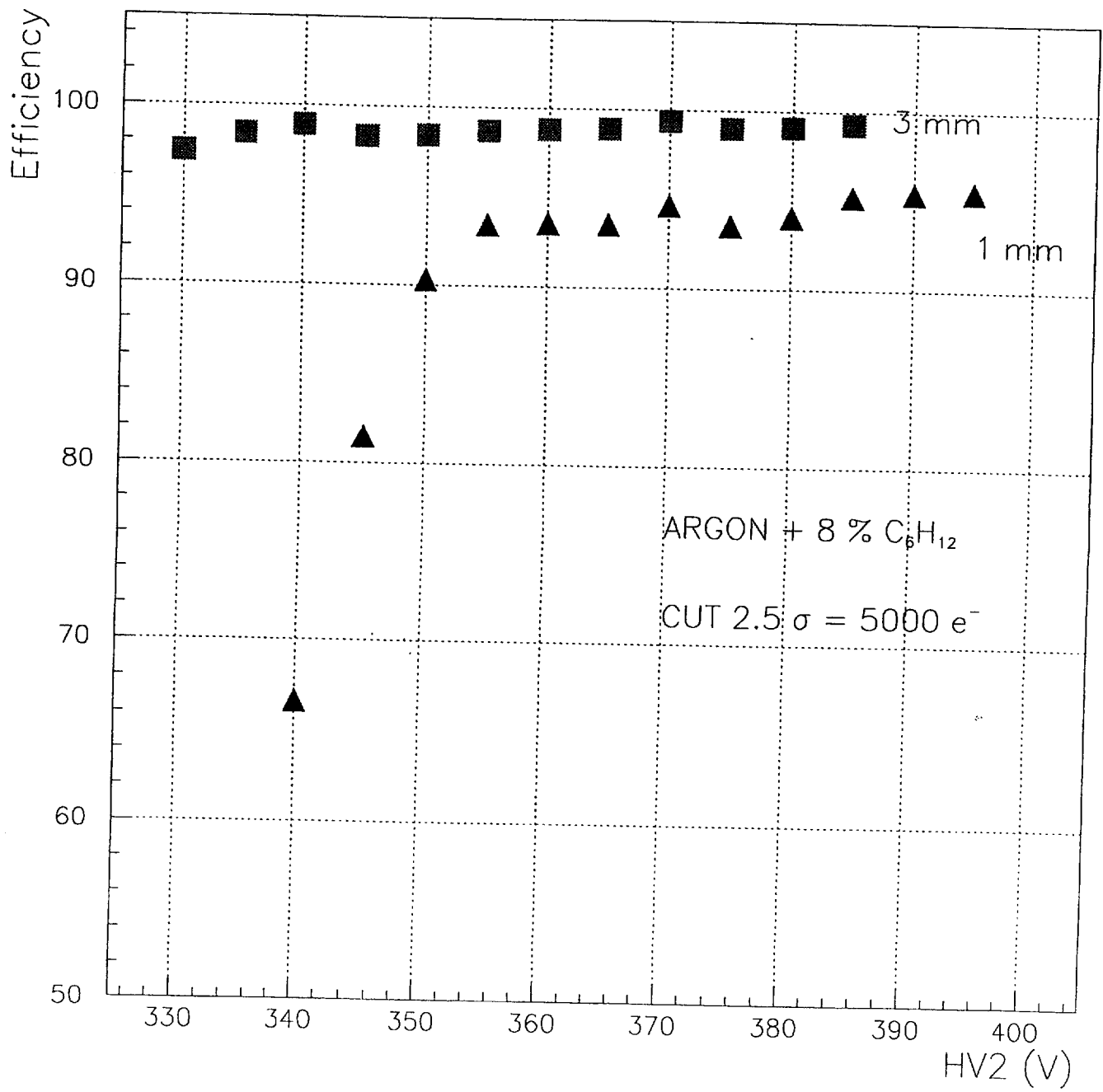


Fig. 15

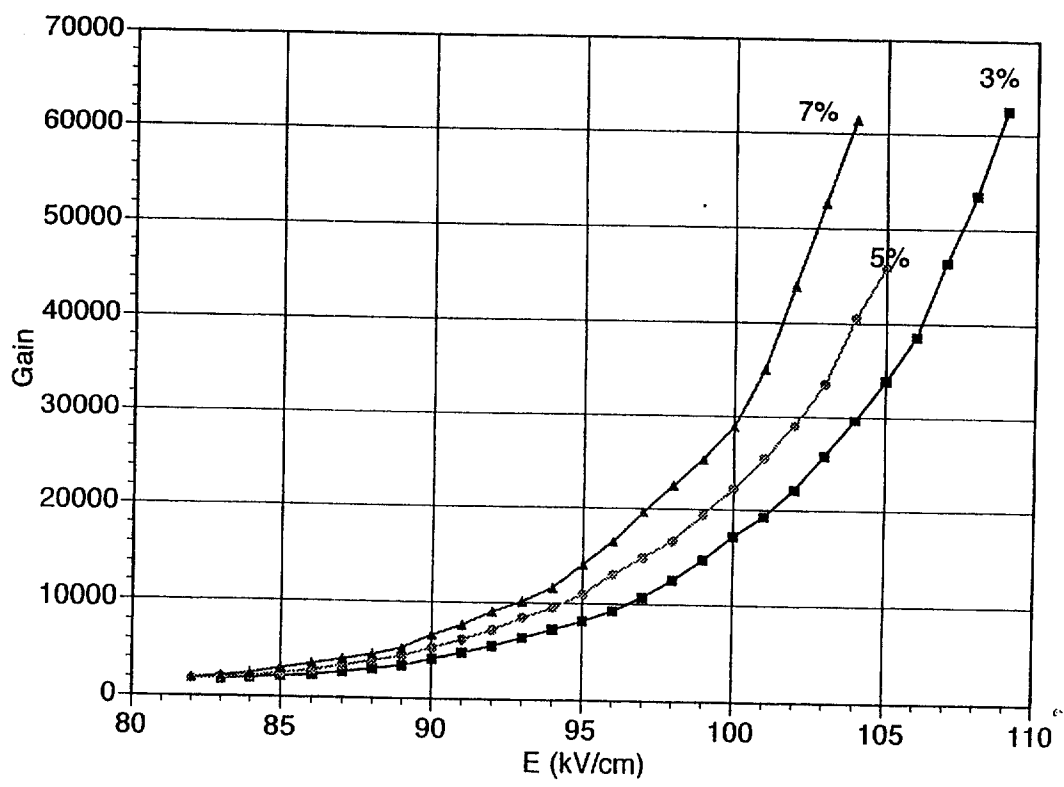


Fig. 16

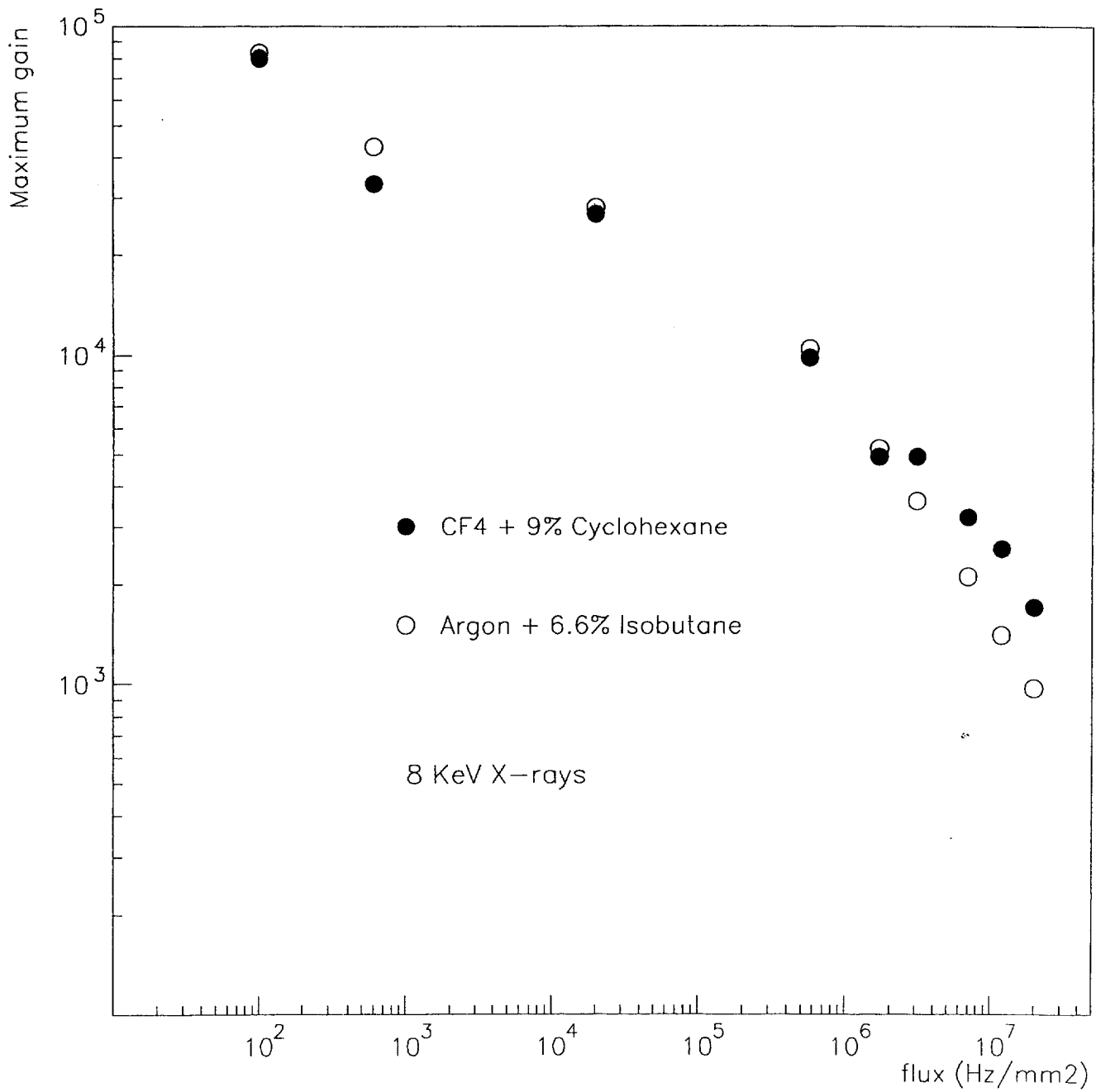


Fig. 17



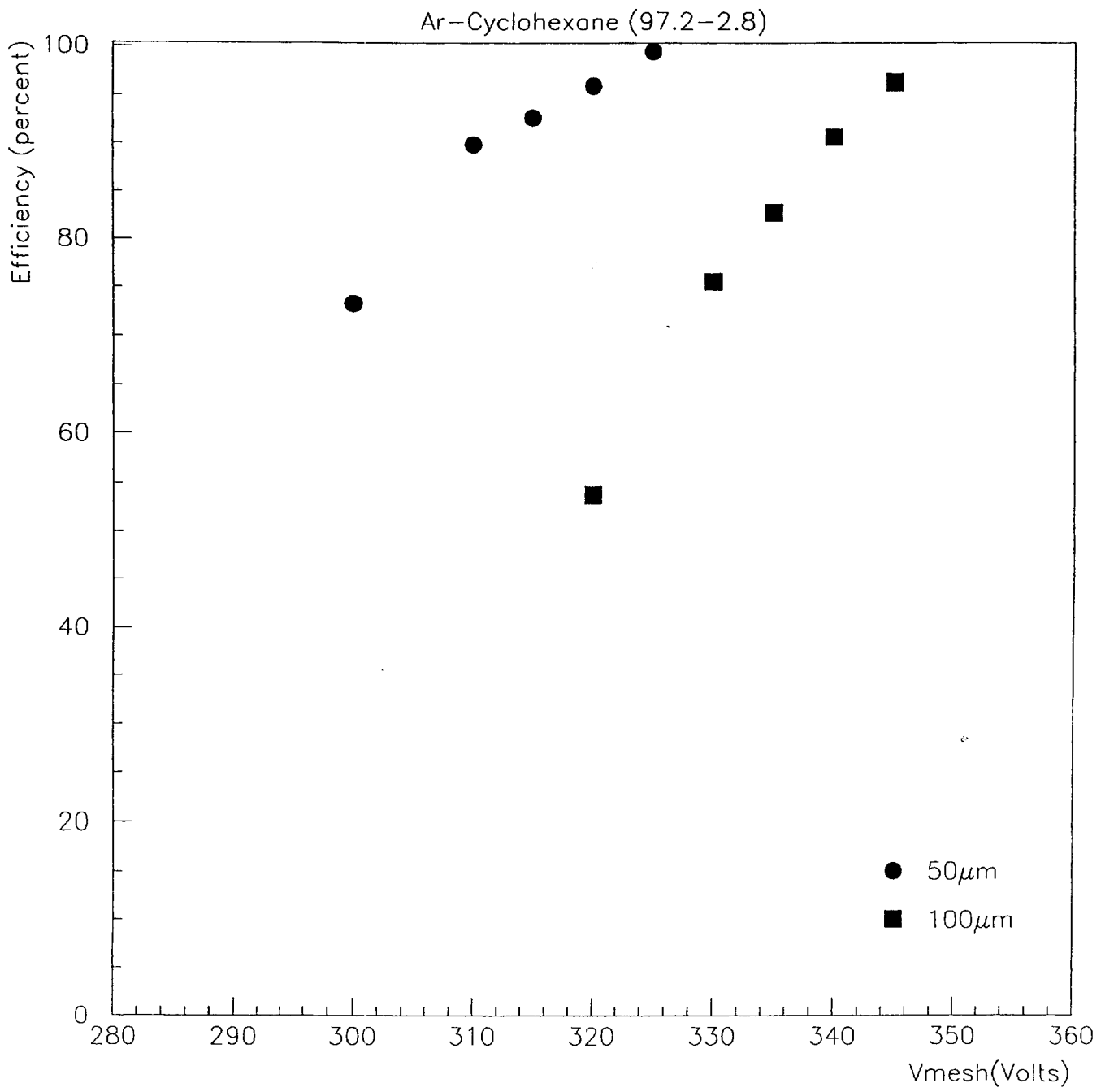


Fig. 18